6th Australasian Hydraulics and
Fluid Mechanics Conference
Adelaide, Australia, 5-9 December 1977

A Comparative Study of the Flow Patterns in Front of Bluff Bodies on the Ground and a Method of their Assessment

J. S. de KRASINSKI
Professor of Mechanical Engineering, University of Calgary, Canada

SUMMARY A Systematic study of separated flows in front of buildings has been undertaken in an atmospheric boundary layer tunnel and in an ordinary one. The data was analysed to develop a semi-empirical method of assessment of the principal distances governing the separating boundary layer patterns on the ground in the front of high rise buildings and of the extent of the "danger zones" subject to high gustiness. The proposed method combined with the phase-plane analysis gives a simple and powerful tool in the hands of architects and town planners.

1 INTRODUCTION

New interest in the environment has brought into focus the topic of separation of atmospheric boundary layers around buildings, which in the wording of classical aerodynamics were listed as "bluff bodies" with little attention being paid to them. Some new approaches have recently appeared fostered by the recent aeronautical interest in separated boundary layers (7). Several authors elaborated in more detail the "phase-plane" method (2,9) which deals rather with a qualitative and kinematic approach leaving the designer with quantitative questions unanswered. This paper is a first step towards bridging this gap and deals with the separation of atmospheric boundary layers in front of buildings.

2 EXPERIMENTAL DATA

2.1 The Wind Tunnels

Wind tunnel A is a classical low turbulence aeronautical, open jet and open circuit wind tunnel with 20" diameter jet in the working section, its velocity is up to 150 fps. A rounded nose protruding board with pressure tappings was built into it, resulting in a thin turbulent boundary layer surrounding the models.

Wind tunnel B is an atmospheric boundary layer wind tunnel, open jet and open circuit. The air after passing through the entrance cone follows a rectangular 4.5'×2.5' channel 48 feet long.

2.2 The Models

Five rectangular sharp edged models were tested. The aspect ratios (height: breadth) covered the typical high rise configurations. The models were placed face to the wind only, their aspect ratios, heights (h), breadths (b) and depths (d) in inches are listed below (Table I).

2.3 Pressure Measurements

The floor pressure tappings provided the information on ground pressures upstream of the models. A special static probe described in (1) was first calibrated and gave very reliable information concerning pressure distribution on the front wall.

TABLE I

Model	h/b	h	b	d
1	.25	2	8	2
2	.5	2	4	2
3	1.0	2	2	2
4	2.0	4	2	2
5	4.0	8	2	2

2.4 Oil Flow Visualization

All the models were analysed using the oil flow visualization technique.

For more details of the experiments see (6).

2.5 Experimental Results

Fig. 1 shows a typical photographic record of a model in the wind tunnel using the oil visualization technique. One clearly observes two distinct patterns in the front related to separation. At the back two foci are clearly seen as well as two saddle lines, one of reattachment and the other of separation. It may be noted that sophisticated methods of analysis of such patterns are now available (2,7.8.9) and an example of such interpretation is shown later.

Figs. 2 and 3 show the pressure distribution in front of the 5 models measured on the ground in the wind tunnels A and B respectively. The pressures are represented by means of the standard pressure coefficient C defined as

$$C = \frac{p - p_\infty}{\frac{1}{2}\rho U_g^2} \qquad (1)$$

where U_g is the gradient height velocity. Subscripts g or h signify measurements on the ground or along the front wall at the height h. Subscript o means the pitot pressure at the stagnation point on the front wall and oMax, the maximum pitot pressure at the stagnation point on the front wall for a very tall building reaching the gradient height. In Table II the separation distances OS_2

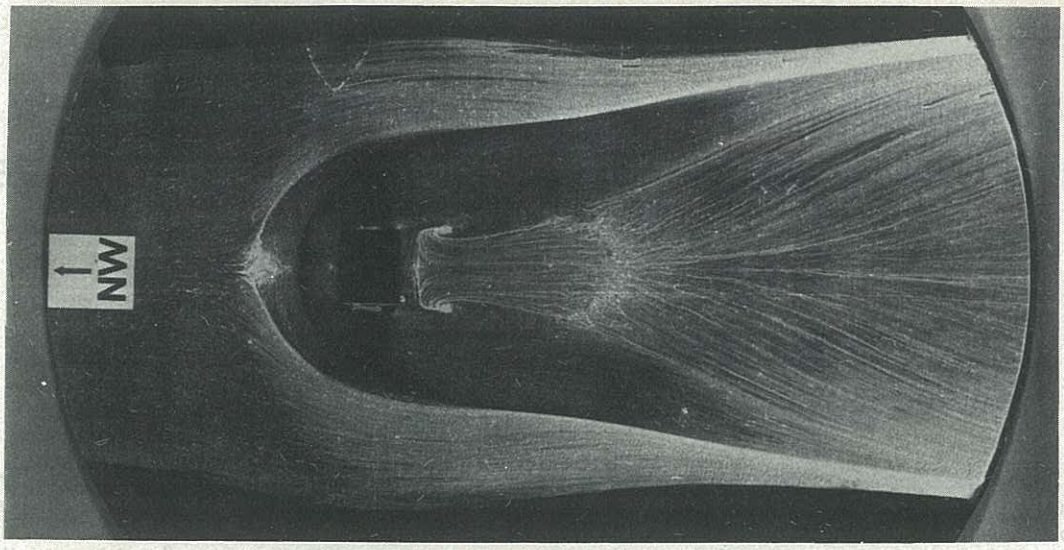

Figure 1 Oil pattern of flow around the model of a building

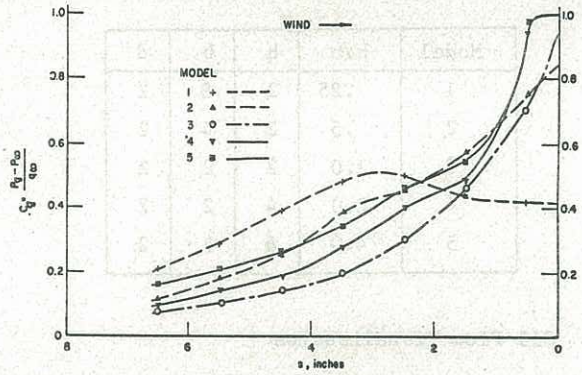

Figure 2 Pressure distribution on the ground Wind Tunnel A

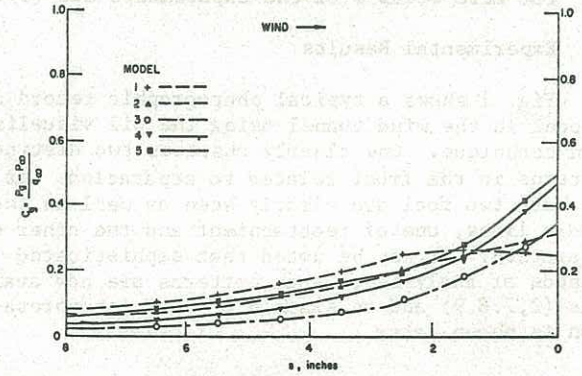

Figure 3 Pressure distribution on the ground Wind Tunnel B

TABLE II

	Wind Tunnel A	Wind Tunnel B
Model	OS_2(in.)	OS_2(in.)
1	1.1	0.88
2	1.23	0.88
3	0.98	0.69
4	1.2	1.0
5	1.11	1.0

are given for the models measured in both wind tunnels.

One observes that for both wind tunnels the differences in ground pressures are rather in terms of intensities than of nature. Thus the separation distances OS_2 are all closer to the building for the case of thick boundary layer in wind tunnel B than for the thin one in A.

Figs. 4 and 5 show the pressure distribution measured on the central line of the front wall, facing the wind, for wind tunnels A and B respectively. One observes that the differences are striking both in intensities and in the nature of the distribution. The maximum value of C_h will be called subsequently C_o. For more details (6) should be consulted.

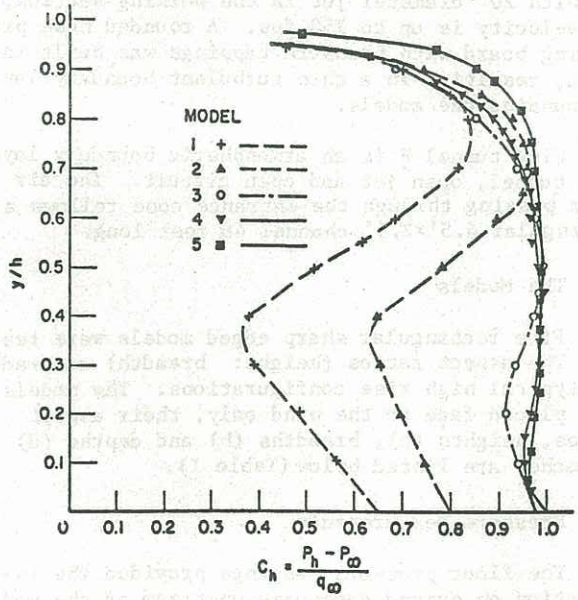

Figure 4 Pressure distribution on the models face Wind Tunnel A

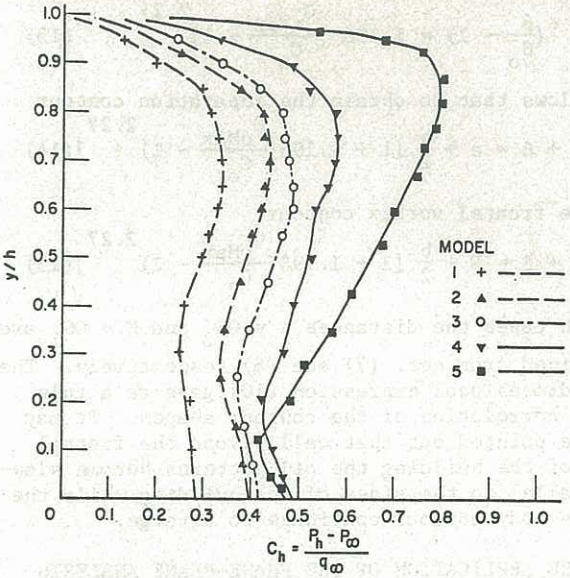

Figure 5 Pressure distribution on the models face Wind Tunnel B

3 THE METHOD OF ANALYSIS

3.1 Initial Physical Considerations

It appears from the collected data that the pressure field in the front of a building facing the wind is governed by the stagnation point pressure at its upper half where a nodal reattachment takes place. If wind tunnel measurements are not available, data from Figure 5 would be useful.

To pursue the argument further one may introduce a new definition i.e. that of pressure velocity U_p related to the pitot pressure on the front wall where

$$U_p = U_g \sqrt{C_o} \qquad (2)$$

is similar to U^* used in the classical description of the turbulent boundary layer. U_p relates to the maximum normal pressure of the pressure field within the boundary layer where separation takes place, as compared to U^*, a measure of the tangential stress on the ground due to turbulence. Obviously the ratio $\frac{U_p}{U^*}$ is a fundamental parameter of similarity in this context.

A second important point in the analysis is the observation that in front of any blunt body standing on the ground a part of the flow returns from the nodal reattachment point into the front of the building and moves upstream within the boundary layer to the point S_2 (Fig. 6) where proper separation occurs. This flow along the face of the building brings to the pedestrian-level high energy eddies. Part of it feeds the vortex sheets produced by the sharp edges of the edifice and another part returns against the main wind direction at the front of the building. It appears from measurements of gustiness at the pedestrian level (4) that its intensity is directly related to the ratio $U_p/U_g = \sqrt{C_o}$. It is of paramount importance for the architect and the designer to be able to determine the "danger areas" where it occurs, and this is the main objective of this paper. This returning flow on the ground is comparable to the source

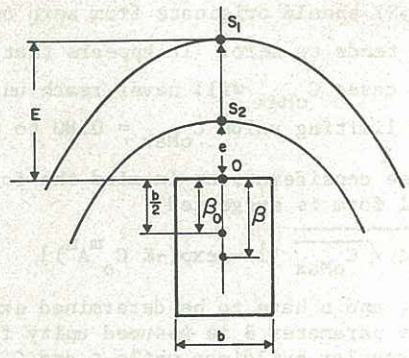

Figure 6 Schematic outline of the separation pattern on the ground

flow in parallel stream of classical hydrodynamics. A detailed analysis of many cases both in low speed and supersonic separation (10,11) confirms this view. The shapes of the oil patterns on the ground are to a great extent practically identical with the Rankine body contours indicating that both phenomena are comparable. The distance to the separation point OS_2 would be determined by the edge of the equivalent Rankine body.

3.2 An Application of the Dimensional Method

From previous discussion it appears that the principal physical parameters upon which depends the distance $e = OS_2$ (Fig. 6) are: the nominal source strength Q, the gradient velocity U_g, the frictional velocity U^*, the pressure velocity U_p, the height of the building h, the gradient height H_g and some unspecified nondimensional shape parameter S. The nominal source strength Q will depend on the intensity of U_p i.e. $Q \sim U_p b^2$ and can be later eliminated. Thus

$$e = f(Q, U^*, h, b, H_g, S) \qquad (3)$$

forming nondimensional groups

$$\frac{e}{\sqrt{\frac{Q}{U^*}}} = f(\frac{h}{H_g}, A, S)$$

where $A = \frac{h}{b}$. Using (2)

$$Q \sim U_p b^2 \sim U_g b^2 \sqrt{C_o}$$

thus

$$\frac{Q}{U^*} \sim \frac{U_g b^2 \sqrt{C_o}}{U^*} \qquad (4)$$

Introducing $\frac{U_g}{U^*} = \zeta = \text{const}$ for a given ground roughness, it follows that

$$e \sim b \sqrt{\zeta \sqrt{C_o}} \cdot f(\frac{h}{H_g}, A, S) \qquad (5)$$

Analysing wind tunnel data it appears that very high aspect ratios combined with high values of h/H_g tending to unity have in the limit very little effect upon the distance OS_2 one is trying to determine and which finally reaches some assymptotic limit while $C_o \to C_{oMax}$. On the other hand the func-

tion $f(h/H_g, A, S)$ should originate from zero once h/H_g and/or A tends to zero. It appears that for all practical cases C_{oMax} will never reach unity but only some limiting value $C_{oMax} = 0.80$ to 0.85.

With these considerations in mind the following functional form is suggested

$$e = \alpha b \sqrt{\zeta \sqrt{C_{oMax}}} \, [1 - \exp(-K \, C_o^{\,m} A^n)] \qquad (6)$$

where α, K, m, and n have to be determined experimentally. The parameter S is assumed unity for standard rectangular buildings while ζ and C_o should be adjusted for each individual case depending upon A, the surrounding roughness and building height as $C_o = f(h/H_g, \zeta, A)$. In this context Fig. 5 would be of assistance if no wind tunnel is available. An analysis of measured data indicates that a good fit is obtained with $\alpha = 0.1$, $K = 2$, $m = 1.0$ and $n = 0.8$, thus (6) becomes

$$\frac{e}{b} = 0.1 \sqrt{\zeta \sqrt{C_{oMax}}} \, [1 - \exp(-2 \, C_o A^{0.8})] \qquad (7)$$

The value of the distance $OS_2 = e$ so estimated has to be fitted into the Rankine body equation.

The distance $E = OS_1$ (Fig. 6) has also been determined in a similar way making use of the observations that $\frac{E}{e} \sqrt[4]{C_o} \simeq$ const. This results in

$$\frac{E}{b} = 0.236 \sqrt[4]{\frac{C_{oMax}}{C_o}} \sqrt{\zeta} \, [1 - \exp(-2 \, C_o A^{0.8})] \qquad (8)$$

3.3 An Application of the Concept of the Rankine Body

From classical hydrodynamics the contour of a two-dimensional Rankine body in polar coordinates is

$$r = r_o \sqrt{\frac{\theta}{\sin \theta}} \qquad (9)$$

and the three-dimensional one is

$$r = \frac{r_o}{\sin \theta} \sqrt{2(1 - \cos \theta)} \qquad (10)$$

where r_o is determined by the source strength Q and velocity U; it represents the distance from the source to the nose of the body. Knowing r_o the shape can be drawn by varying θ. If the distance from the source to the front edge of the building is β, (Fig. 6) then

$$r_o = \beta + e \qquad (11)$$

is required to draw the separation contour. For very tall buildings $\beta \to b/2 = \beta_o$. Similarly for the determination of the frontal vortex, saddle contour

$$r_o = \beta + E \qquad (12)$$

For decreasing aspect ratios and/or low buildings the edge of the separating line follows closely the front edge of the edifice with a substantial increase in the radius of curvature thus in the limit $\frac{\beta}{\beta_o} \to \infty$.

A good correlation has been obtained in the form

$$\left(\frac{\beta}{\beta_o} - 1\right) = 1.196 \left[\frac{C_{oMax}}{C_o} - 1\right]^{2.27} \qquad (13)$$

It follows that to obtain the separation contour

$$r_o = e + \beta = e + \frac{b}{2} \left[1 + 1.196\left(\frac{C_{oMax}}{C_o} - 1\right)^{2.27}\right] \qquad (14)$$

and the frontal vortex contour

$$r_o = E + \beta = E + \frac{b}{2} \left[1 + 1.196\left(\frac{C_{oMax}}{C_o} - 1\right)^{2.27}\right] \qquad (15)$$

In both cases the distances $e = OS_2$ and $E = OS_1$ are determined from eqs. (7) and (8) respectively. The three-dimensional expression (10) gave as a rule better correlation of the contour shapes. It may also be pointed out that well beyond the frontal edges of the building the oil patterns become slowly parallel to the sides of the building while the Rankine body contour continues to diverge.

4 THE APPLICATION OF THE PHASE-PLANE ANALYSIS COMBINED WITH THE PROPOSED METHOD

4.1 Introductory Remarks

It is not the object of this paper to discuss the phase-plane technique and the reader is referred to the literature (2,3,7,9). Without counting the "principal nodes" the amount of nodes and saddles is equal. Also vector rotations around such singularities follow rigid laws. This particular point, in relation to wind tunnel work has been developed by J Hunt (2). It appears that saddles, nodes and foci on the ground (XY plane) are associated with rotations -2π, 2π and 2π respectively. When observed at the ground level in the XZ plane the saddles and nodes are associated with $-\pi$. The important point is that each field, say in the front and at the back of a building must have its total rotation balanced in such a way that it is finally zero. This is illustrated in the following example.

4.2 Illustrative Example

For a tall building staying in the open some typical roughness height or the equivalent U_g/U^* must be assessed as well as the value of the frontal stagnation point coefficient C_o. Knowing the building geometry eqs. (7), (8), (10), (14) and (15) give quick method to draw the contours around the building within which intense gustiness would be present. Once the distances OS_1 and OS_2 have been determined the phase-plane method can be successfully applied and a pattern similar to the one in Figures 7a and 7b can be drawn.

5 CONCLUSIONS

A semi-empirical method has been developed based on wind tunnel measurements, and dimensional analysis to determine the fundamental distances of separating patterns in front of the buildings. Advantage was also taken of the fact that such patterns follow closely the shapes of Rankine body in uniform flow. A new concept has been introduced: that of "pressure velocity" U_p, i.e. the velocity of the streamline which reaches the stagnation point at the front of the building.

6 ACKNOWLEDGEMENTS

The help of the Canadian National Research Council is gratefully acknowledged.

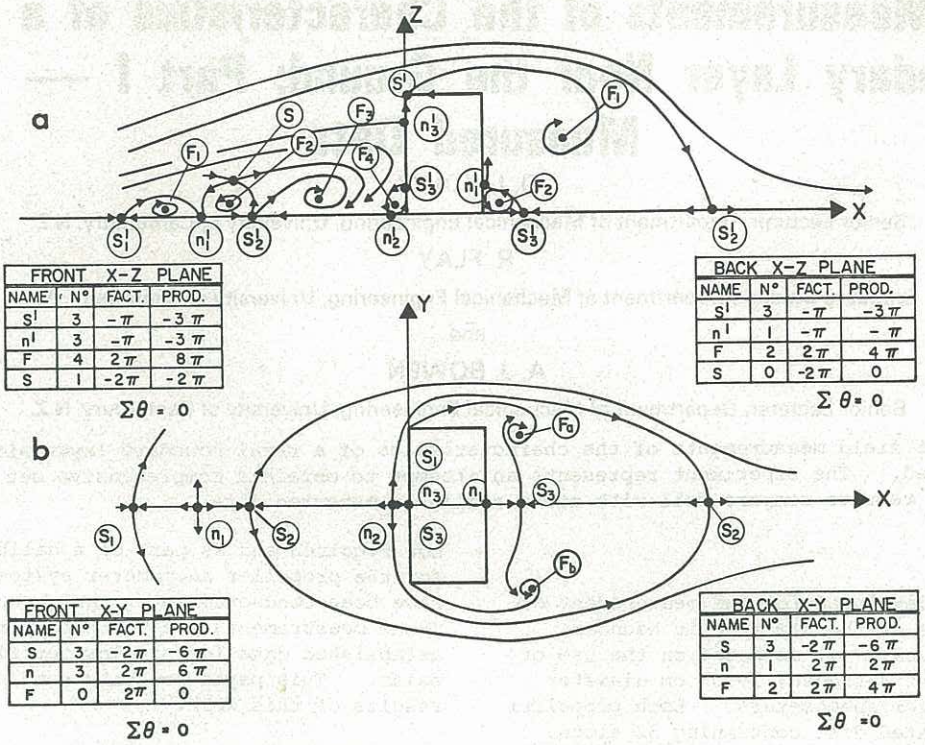

Figure 7 Suggested flow and separation patterns (not to scale) related to Figure 1

7 REFERENCES

1 CHASTEAU, V. A. (1974). A probe for the rapid measurement of surface static pressure distribution. Fifth Australian Conference on Hydraulics and Fluid Mechanics.

2 HUNT, J. (1974). Notes on visualizing the mean flow field around a three-dimensional surface obstacle in a turbulent flow. Unpublished report, The University of Cambridge, courtesy of the author.

3 KAPLAN, W. (1958). Ordinary differential equation. Addison-Wesley, Chapter XI.

4 de KRASINSKI, J. and ANSON, W. (1976). Wind tunnel measurements of flow around the Rank City Wall Phase II project. Report 78a and 78b, Department of Mechanical Engineering, The University of Calgary.

5 LEUNG, R. and de KRASINSKI, J. (1973). Comparison between wind tunnel oil visualization and full scale measurements of the campus of the University of Calgary. Report 50, Department of Mechanical Engineering, The University of Calgary.

6 LEUNG, R. (1976). A study of the separation of flow and pressure distribution in front of the buildings. M.Sc. thesis, Department of Mechanical Engineering, The University of Calgary.

7 LIGHTHILL, M. J. (1963). Laminar boundary layers. Oxford University Press (Ed. L. Rosenhead), Chapter II.

8 OSWATITSCH, K. (1957). Die Ablosungsbedingung von Grenzschichten. IUTAM Symposium, Freiburg i, Br. (Görtler Ed.).

9 PERRY, A. and FAIRLIE, B. (1974). Critical points in flow patterns. Advances in Geophysics, 18, B.

10 ZUBKOV, A., YU, A., PANOV, D. and VOYTENKO, M. (Moscow) (1967). Supersonic gas flow about the cylinder on a flat plate. Fluid Mechanics Transactions, 3, pp. 627-638.

11 ZUBKOV, A., YU, A., PANOV, D. and VOYTENKO, M. (Moscow) (1970). On flow patterns ahead of obstacles at supersonic speeds. Fluid Dynamics Transactions, Vol. 5, Part I, pp. 229-307. Institute of Fundamental Technical Research, Polish Academy of Sciences.